Folliculogenesis and ovulation in fish are controlled by distinct neuropeptides

Lian Hollander Cohen[1], Miriam Shulman[1], Pierre Fontanaud[2,3], Omer Revah[5], Patrice Mollard[2,3], *Matan Golan[4] & *Berta Levavi Sivan[1].

(1) Department of Animal Sciences, The Robert H. Smith Faculty of Agriculture, Food, and Environment, Hebrew University of Jerusalem, Rehovot 76100, Israel.

(2) Institute of Functional Genomics, University of Montpellier, CNRS, INSERM, France.

(3) BioCampus Montpellier, University of Montpellier, CNRS, INSERM, F-34094 Montpellier, France.

(4) Department of Poultry and Aquaculture, Institute of Animal Sciences, Agricultural Research Organization, Volcani Center, P.O.B 15159, Rishon Letziyon 7505101, Israel.

(5) The Koret School of Veterinary Medicine, The Hebrew University of Jerusalem, Jerusalem, Israel

Abstract

Many fish species display clear temporal separation between prolonged periods of energetically costly gonadal development, and short spawning events. These two distinct processes are controlled by the gonadotropins follicle-stimulating hormone (FSH) and luteinizing hormone (LH), respectively. While it was suggested that a common secretagogue, gonadotropin-releasing hormone (GnRH), controls both functions, it is unclear how the secretion of the two gonadotropins is differentially regulated. Here, we used *in vivo* and *ex vivo* calcium imaging of zebrafish gonadotrophs to study the regulation of gonadotropin release in fish. We show that while LH cells are highly responsive to GnRH stimulation, the response of FSH cells is weak and inconsistent. By combining transcriptomics and calcium imaging, we found that FSH cells express the receptor for the satiety hormone cholecystokinin (CCK) and display a strong calcium response to its application, accompanied by FSH secretion, which designates this peptide as a *bona fide* FSH secretagogue. From an evolutionary perspective, these findings indicate that the control of folliculogenesis and ovulation in fish was placed under different neural circuits, which respond to the specific somatic and environmental cues relevant to each process.

1. Introduction

Egg-laying and placental animals display a marked difference in their reproductive energy allocation strategies. In oviparous species, the preovulatory processes of gonadal development and yolk deposition into the developing oocyte, also known as folliculogenesis, constitute the main nutritional challenge during the female reproductive cycle. By contrast, in placental mammals, post-ovulatory pregnancy and milk production require recruitment of the maternal metabolic pathways to accommodate the nutritional needs of the offspring. Thus, in oviparous species, folliculogenesis is gated by the nutritional status of the animal, whereas in mammals, poor nutrition mainly restricts ovulation (1, 2).

The dependence of folliculogenesis on nutrition is particularly apparent in fish. In this most ancient and diverse group of living vertebrates, most species exhibit long periods of nutritionally-demanding folliculogenesis, followed by little to no parental care of the offspring. In extreme cases, such as in salmon, folliculogenesis may span years and culminate in a single spawning event during the entire lifespan of the animal (3).

The process of gonadal growth is also important for aquaculture, as it constitutes a major bottleneck in the life cycle of many commercial fish species (4). Nevertheless, while hormonal treatments are used mainly to overcome reproductive failures during the final stages of gonadal development, such as ovulation and spermiation (5-10), there are no efficient treatments for impaired folliculogenesis and gonad growth.

In all vertebrates, the processes of folliculogenesis and ovulation are controlled by two gonadotropin hormones (GtH), follicle-stimulating hormone (FSH) and luteinizing hormone (LH), respectively. Secretion of both these GtHs by gonadotrophs of the anterior pituitary gland is controlled by the hypothalamic neuropeptide gonadotropin-releasing hormone (GnRH), which is produced by a small population of neurons in the preoptic area (11). Studies conducted in mammals have shown that the differential control over gonadotropin secretion is attained via changes in frequencies and amplitude of GnRH pulses, as well as by a variety of other endocrine and paracrine factors that dictate whether the cells will secrete LH or FSH (12-14). However, the mechanism governing the differential release of FSH or LH in other vertebrates remains largely unknown.

In fish, the function of gonadotropins is highly stereotyped, as FSH signalling strictly controls folliculogenesis whereas the role of LH is restricted to the induction of ovulation (15, 16). As in mammals, GnRH is considered the master regulator of gonadotropin secretion in fish. Yet, in recent years, its status as the sole neuropeptide regulating GtH secretion has been called into question, as other hypothalamic neuropeptides were shown to bypass GnRH and directly regulate gonadotropin secretion (17-22). Moreover, the effects of GnRH seem to be limited to the control of final oocyte maturation and ovulation via LH secretion (15). The hypothalamic factor controlling FSH secretion and, thereby, folliculogenesis in fish has yet to be identified.

Here, we addressed the question of the differential control of LH and FSH secretion in fish. For that, we combine transcriptomics, *in vivo* and *ex vivo* calcium imaging in fish gonadotrophs to identify LH- and FSH-specific secretagogues. We show that the two types of gonadotrophs vary significantly in their activity patterns. Moreover, we show that whereas LH cells are predominantly controlled by GnRH, FSH cells are preferentially activated by the satiety hormone cholecystokinin (CCK), which is also produced in the fish brain (23, 24), providing a direct link between nutritional status and gonadal development. These separate regulatory circuits underlie the distinct secretion patterns of FSH and LH and thereby allow differential control of folliculogenesis and ovulation in fish.

2. Results

LH and FSH cells exhibit distinct calcium activity *in vivo*

Whereas in mammals, both LH and FSH are secreted by the same cell population, in fish, these gonadotropins are produced by discrete cell types (25). This feature provides a unique opportunity to identify genes and pathways that specifically regulate the two gonadotropins. To that end, we generated transgenic zebrafish in which both LH- and FSH-producing cells express the red genetically-encoded calcium indicator RCaMP2 (26), whereas FSH cells also express GFP (Tg (FSH:RCaMP2; LH:RCaMP2; FSH:GFP); Fig. 1a). These fish allow to simultaneously distinguish between LH and FSH cells and monitor calcium activity, as a readout for cell activation and gonadotropin secretion, in both cell types.

To follow the activity of LH and FSH gonadotrophs in live fish, we developed a novel preparation for imaging the pituitary gland at single-cell resolution while maintaining the *in vivo* context. In this preparation, the pituitary gland was exposed from its ventral side by the removal of the lower jaw. The immobilized fish was placed under a two-photon microscope with a constant flow of water over the gills (Fig. 1b), ensuring sufficient oxygen supply to the fish and blood flow to the gland (Supplementary Movie 1 shows blood flow in pituitary blood vessels).

Examination of the two gonadotroph cell types revealed distinct types of calcium activity (Fig. 1 c-e). While LH cells were mostly silent, FSH cells exhibited short (mean of 10.08 sec half width) calcium bursts (mean of 0.6 $\Delta F/F$; Fig 1c fish1 and d). Theses calcium events were sparse, i.e. between 1 and 7 transients in each cell in 10 min, and disorganized, as cross-correlation coefficient values ranged from 0.3 to 0.9 (Fig. 1e fish1, Supplementary Movie 2b). In 7/10 fish we observed a different type of calcium activity, in which LH cells exhibited a single long (mean of 75.55 sec half width) and strong (mean of 1.5 $\Delta F/F$) calcium rise (Fig. 1c fish2 and d). This event was synchronized between LH cells (mean cross-correlation values of 0.9 ± 0.01) and, in 3/7 fish, it was followed by a less synchronized (mean cross-correlation values, 0.66 ± 0.03) calcium rise in FSH cells (Fig. 1c and e fish2, Supplementary Movie 2a). On average, the cross-correlation coefficient values of all active LH cells were significantly higher compared to FSH cells (Fig. 1e, Supplementary Figure 1b), which reflects the stronger coupling between LH cells (25). Delay analysis showed a clear temporal and spatial activation pattern of LH cells, where neighbouring cells exhibited a shorter delay in

activation. In contrast, FSH cells displayed less spatially organized activation patterns with longer delay values (Fig. 1e). We did not observe significant sexual dimorphism in correlation levels in either LH or FSH cells (p_{LH}=0.42, p_{FSH}= 0.057, 5 males and 5 females, Supplementary Figure 1b). While in some cases LH cell activation was accompanied by a calcium rise in FSH cells, most FSH calcium transients were not associated with a rise in calcium in LH cells. We therefore speculated that a cell type-specific regulatory mechanism drives the activity of FSH cells.

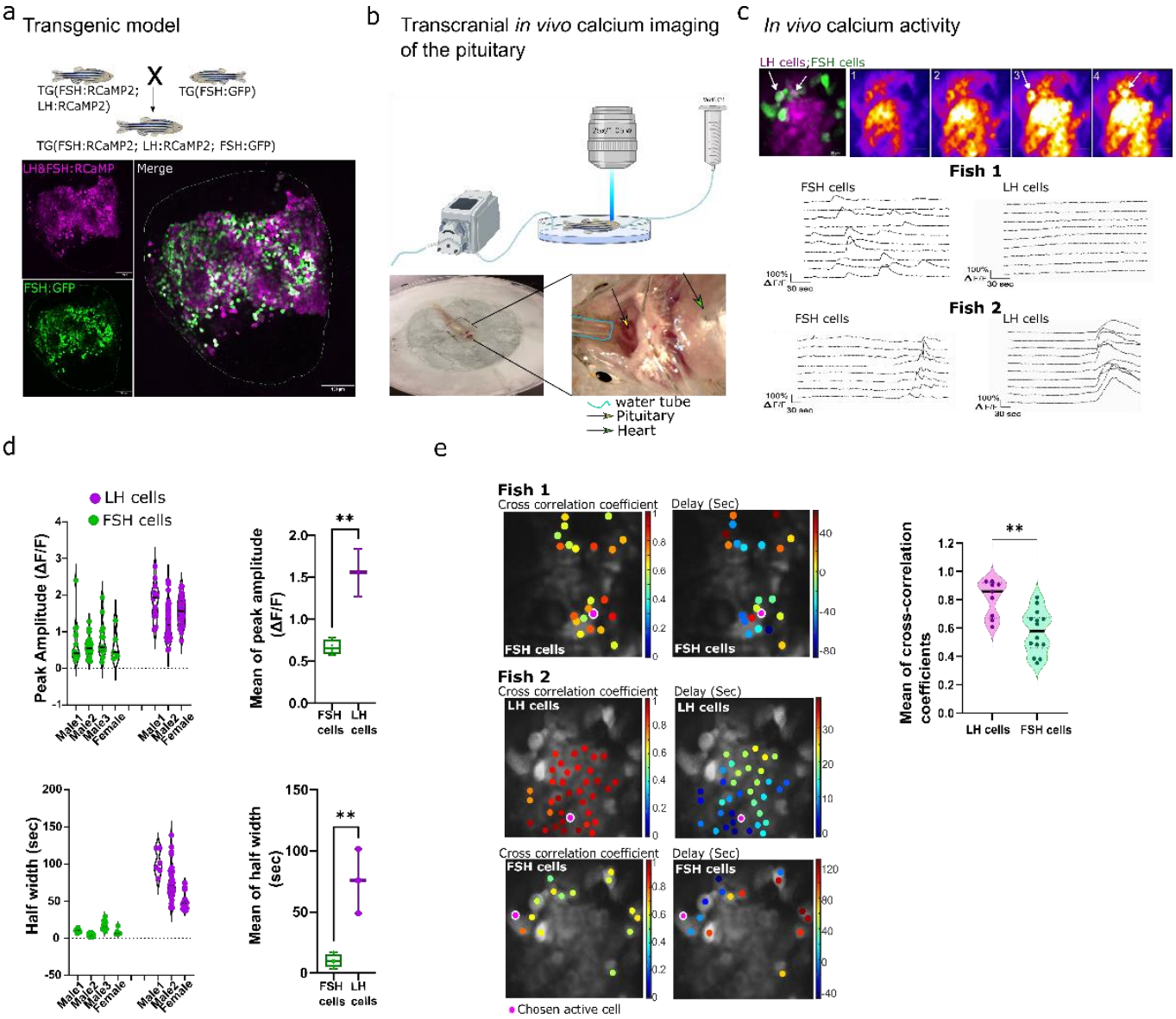

Figure 1. LH and FSH cells exhibit distinct spontaneous activity patterns *in vivo*

(a) Triple transgenic fish were generated by crossing transgenic fish expressing GFP in FSH cells, and fish expressing R-CaMP2 in LH and FSH cells. Bottom: A confocal image of the pituitary shows RCaMP2 expression in both cell types and GFP expression in FSH cells.

(b) A diagram describing the setup of the *in vivo* experiments. Bottom images show the mounted fish after the pituitary was exposed ventrally; arrows indicate the pituitary and heart.

(c) A representative image of *in vivo* calcium activity (see Supplementary Movie 2). On the top left is a merged image depicting FSH cells in green and LH cells in magenta. The other top panels show sequential calcium imaging, which reveals calcium rise in all LH cells followed by calcium rise in FSH cells (marked by green arrows). The bottom panels show the calcium traces (ΔF/F) of LH and FSH cells in two different imaged pituitaries, one where only FSH cells were active (Fish 1) and another where both cell types were active (Fish 2).

(d) Graphs showing properties of spontaneous calcium transients (ΔF/F) in LH cells and FSH cells in three males and one female. Means of peak amplitude and duration differed between LH and FSH cells (unpaired *t*-test, * $p<0.05$, ** $p<0.001$). Analysis was performed using pCLAMP 11.

(e) Left: An example of calcium analysis performed on imaged pituitaries. The color-coded data points were superimposed on the imaged cells and represents the maximum cross-correlation coefficient or the delay between a calcium trace of a region of interest (ROI) and that of the rest of the cells in the same population. The delay map of Fish 2 show that during the calcium rise, all LH cells exhibited highly correlated calcium traces that were organized temporally and spatially, starting from the bottom left and moving to the top right. In comparison, the activity of FSH cells was either synchronized (e.g. Fish 2) or disorganized (Fish 1). Graph on the right summarizes the coefficient values of repeated *in vivo* calcium imaging assays (n=14, see Supplementary Fig. 1 for all measurements). The values for LH cells are significantly higher and more uniform than those of FSH cells (unpaired *t*-test, * $p<0.05$, ** $p<0.001$).

GnRH primarily activates LH cells

Next, we sought to characterize the response of the cells to GnRH, their putative common secretagogue. To determine the effect of GnRH on gonadotroph activity, we utilized an *ex vivo* preparation that preserves the brain-pituitary connection intact (Fig. 2a-b). Without stimulation, LH cells were either silent or exhibited small and short calcium transients (2-8.8 sec half width, amplitude 0.23 -0.66 ΔF/F; 7/10 fish; Fig. 2C, Supplementary Movie 3a-a', Supplementary Figure 2), which were synchronized between small groups of neighbouring cells (2-14 cells per fish with a cross-correlation > 0.5, 0>delay>0.25, Supplementary Figure 3). Regardless of the basal activity of LH cells, in 80% of the fish, FSH cells elicited short and strong calcium bursts that had no clear organization in time or space, similar to the unorganized calcium events observed *in vivo* (5.8-12.13 sec half width, amplitude 0.63 - 1.03 ΔF/F; Fig. 2C, Supplementary Figure 2, Supplementary Movie 3c-c').

For stimulation, we applied a GnRH analogue used for spawning induction in fish (27). In response to GnRH stimulation, LH cells exhibited a strong and slow calcium rise (average half width 48.6 sec and average amplitude of 1.99 ΔF/F; Fig. 2d, Supplementary Figure 2, Supplementary Movies 3a'' and b-b'), which was synchronized between the cells, as observed by the increase in correlation values from 0.31 ± 0.11 to 0.7 ± 0.13 (Fig. 2e-f). In contrast, FSH cells showed a significantly lower and more variable response rate. Only 50% of the fish displayed an increase in cross-correlation values from the basal state (Fig. 2e), which was not statistically significant (Fig. 2f). Overall, whereas GnRH elicited response in 95% of LH cells, only 56% of FSH cells responded to the treatment (Fig. 2g). Due to this inconsistent response of FSH cells to GnRH stimuli we speculated that a different neuropeptide regulates their activity.

a Brain-pituitary *ex vivo* preperation

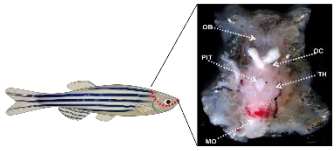

b *Ex-vivo* confocal imaging

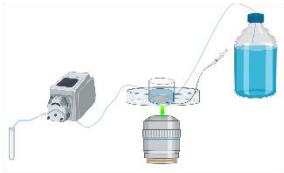

c Basal activity of gonadotrophs

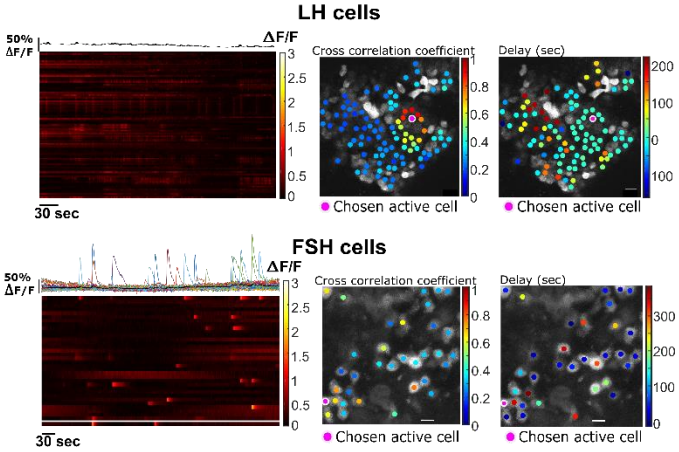

d GnRH-stimulated activity of gonadotrophs *ex vivo*

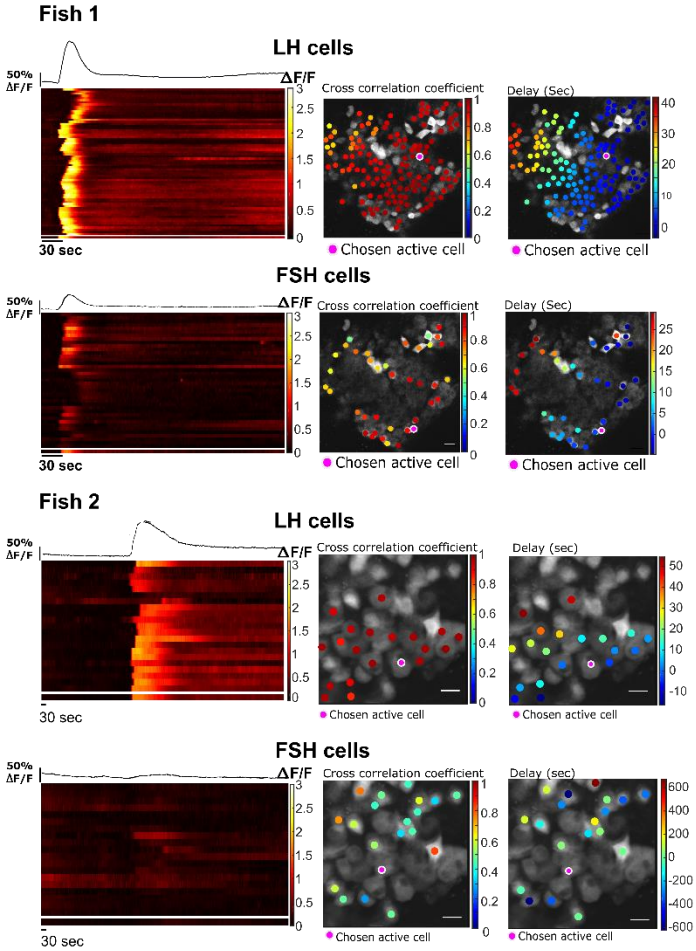

e Cross correlation values in stimulated and non stimulated cells

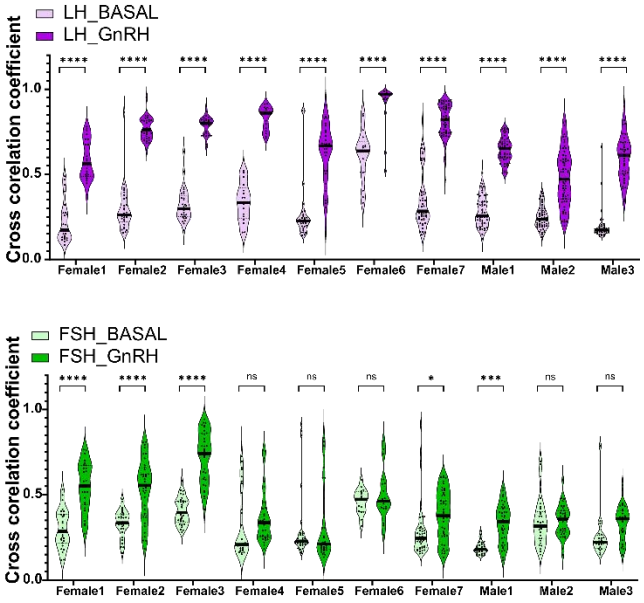

f Comparing the mean of all cross correlation values

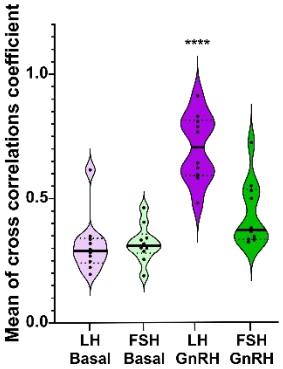

g Percentage of responding cells

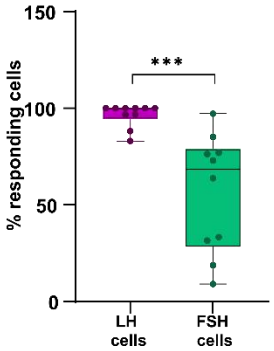

Figure 2. GnRH induces a synchronized increase of calcium in all LH cells

(a) Image of a dissected head with pituitary exposed from the ventral side of the fish used for the *ex vivo* assays (OB, olfactory bulb; OC, optic chiasm; PIT, pituitary; TH, thalamus; MO, medulla oblongata).

(b) A diagram describing the *ex vivo* setup with a constant flow of artificial cerebrospinal fluid (ACSF), a side tube to inject stimuli, and a collecting tube.

(c) A representative analysis of basal calcium activity of LH and FSH cells. The left panel is a heatmap of calcium traces (ΔF/F), where each line represents a cell, with the mean calcium trace on top. The color-coded data points on the right are superimposed on the imaged cells and represent the maximum cross-correlation coefficient or the delay between a calcium trace of an active ROI to those of the rest of the cells in the same population. LH cells exhibited short calcium rises that were correlated in pattern and time between small groups of cells, whereas short, unorganized calcium transients were observed in FSH cells (see Supplementary Fig. 2 for additional cell activity parameters).

(d) An analysis of calcium response to GnRH stimulation in two representative imaging sessions. In all LH cells, a significant calcium rise was highly correlated and temporally organized, as the closest cells had a shorter delay. In 5/10 fish, a similar response to the stimulus was seen in FSH cells, albeit with lower calcium intensities and coefficient values (e.g., Fish 1) whereas in the other 5 fish FSH cells did not respond at all (e.g., Fish 2).

(e) Comparison of basal calcium activity to calcium response during GnRH stimulation. In all the fish (n=10), coefficient values of LH cells (top) were significantly higher than baseline values. In FSH cells (bottom), only 50% of the fish showed a significant rise in response to GnRH (one-way ANOVA, * $p<0.05$, ** $p<0.001$).

(f) The mean cross-correlation coefficient values in each cell type (from e) under each treatment reveal that only LH cells are significantly affected by GnRH stimuli (two-way ANOVA, * $p<0.05$, ** $p<0.001$).

(g) The percentage of cells responsive to GnRH stimulus (i.e., coefficient values higher than the 80 percentiles of basal values) is significantly higher in LH cells compared to FSH cells. Each dot represents one fish (unpaired *t*-test, * $p<0.05$, ** $p<0.001$).

CCK directly activates FSH cells

In search for a neuropeptide other than that may serve as FSH secretagogue in fish, we examined the possible involvement of CCK. While three types of CCK receptors (CCKRs) are reported in the genome of fish, only one type is expressed in the pituitary gland (28). This receptor is also the most abundant in FSH cells, where its expression is ~100 fold higher than in LH cells (Fig. 3a). We therefore first validated its specific expression on FSH cells in zebrafish using *in situ* hybridization (Fig. 3b). Moreover, using immunohistochemistry, we showed that CCK-secreting hypothalamic neurons are hypophysiotropic. Neuronal projections expressing this peptide were identified innervating the pituitary near FSH cells and adjacent to GnRH axons (Fig. 3c), indicating hypothalamic input of CCK into the pituitary gland. To functionally test the effect of CCK on gonadotroph activity, we applied the peptide (250 µl of 30 µg/ml CCK) to our *ex vivo* preparation and monitored the calcium response of the cells. Results showed that CCK elicited a strong calcium response (40.3 to 172 sec half width, mean amplitude of 1.44 ΔF/F) specifically in FSH cells (Fig. 3e, Supplementary Figure 2, Supplementary Movie 4). In all analysed fish, all FSH cells responded to CCK, whereas the number of LH cells that responded to the stimulation varied widely (20%-100%, n=6; Fig. 3g). The calcium response in FSH cells was highly synchronized (mean cross-correlation coefficient, 0.73±0.038; Fig. 3d-f) with a clear spatial and temporal organization (Fig. 3d). By contrast, the response of LH cells to CCK application was characterized by low cross-correlation coefficient values (0.46±0.054; Fig. 3d-f). Mean cross-correlation values were significantly elevated in response to the stimulation only in FSH cells (1.6 vs 3-fold change in LH and FSH cells, respectively; Fig. 3f). These results indicate that in fish, FSH cells are predominantly activated by CCK.

a Expression of GnRH and CCK receptors in tilapia gonadotrophs

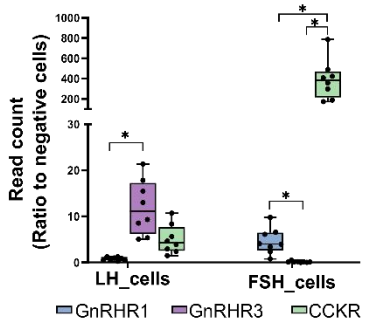

b Expression of CCK receptor in zebrafish gonadotrophs

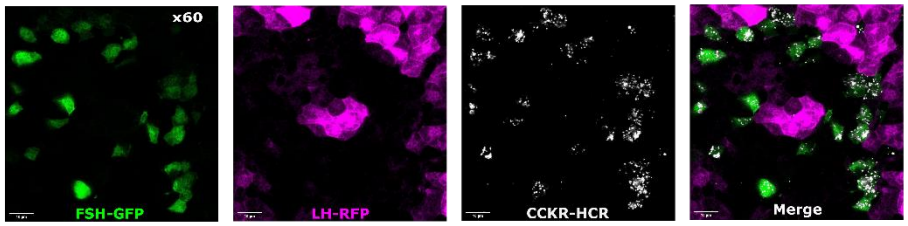

c CCK-producing axon innervate the pituitary

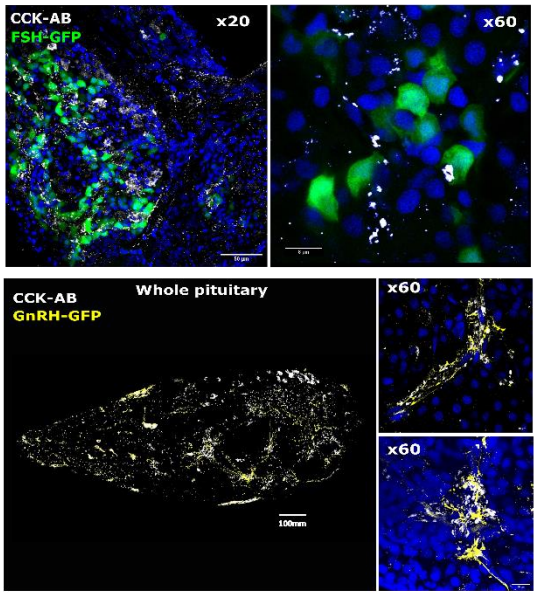

d Stimulation of gonadotrophs by CCK

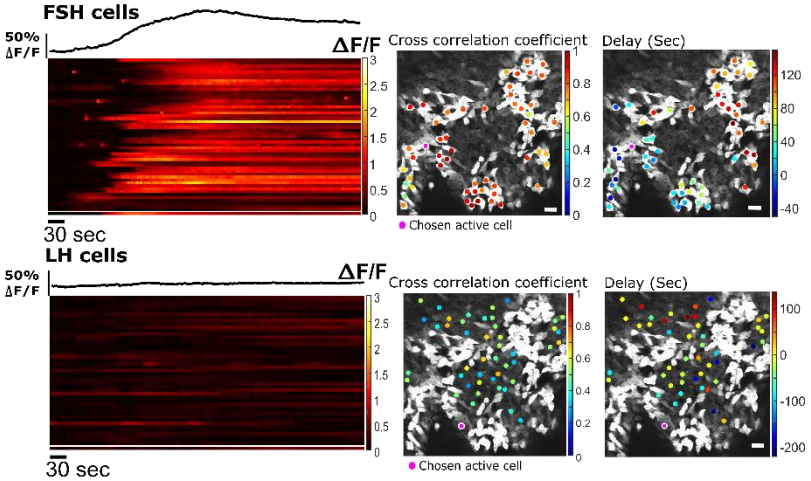

e Cross correlation values in stimulated and non stimulated cells

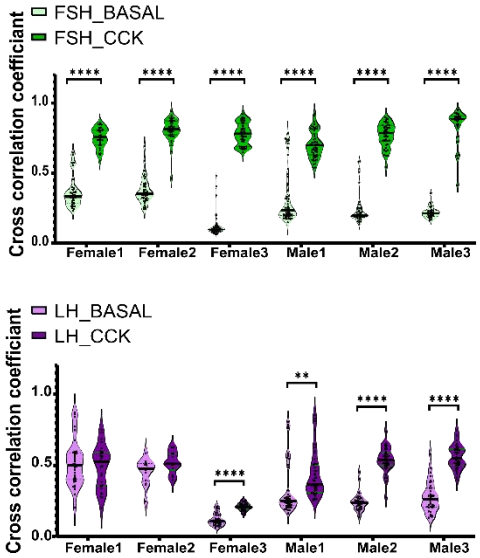

f Comparing the mean of all cross correlation values

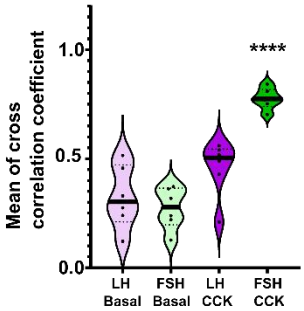

g Percentage of responding cells

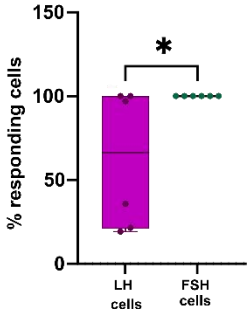

Figure 3. FSH cells are directly stimulated by CCK

(a) Expression of CCKR and two identified GnRH receptors in LH and FSH cells. Expression data were taken from a transcriptome of sorted pituitary cells of transgenic Nile tilapia (*Oreochromis niloticus*), expressing RFP in LH cells and GFP in FSH cells, previously obtained by Hollander-Cohen *et al (28)*. Each dot represents a FACS fraction from a bulk of 20 pituitaries (n=8, 4 groups of males and 4 groups of females). The expression of each gene in each cell type is normalised to its expression in non-gonadotroph pituitary cells. While GnRHR3 is the dominant receptor in LH cells, CCKR has a significantly higher expression in FSH cells (two-way ANOVA, * $p<0.05$, ** $p<0.001$).

(b) Hybridization chain reaction (HCR) for CCKR (white) on transgenic zebrafish pituitaries expressing RFP in LH cells (magenta) and GFP in FSH cells (green) shows specific expression only on FSH cells.

(c) Immunohistochemical staining of CCK in transgenic fish expressing GFP in FSH cells (top panel) or GFP in GnRH neurons (bottom panel). The CCK neuronal axons that innervate the pituitary gland are located adjacent to GnRH axons and in very close proximity to FSH cells.

(d) Calcium analysis of FSH and LH cells during CCK stimulation. The left panel is a heatmap of calcium traces ($\Delta F/F$), where each line represents a cell. On top of the heatmap is a graph showing the mean calcium trace and on the right are color-coded data points that are superimposed on the imaged cells, showing the maximum cross-correlation coefficient (left) and the delay between a calcium trace of an active ROI and those of the rest of the cells in the same population. A high calcium rise (2.5 $\Delta F/F$) was observed in FSH cells, with high coefficient values (mean, 0.75 ± 0.07) and a clear pattern of a delay moving from left to right. LH cells did not respond to the stimulus, displaying low coefficient values (mean, 0.49 ± 0.15) and no spatial organization of the delay.

(e) Comparison of basal and CCK-stimulated calcium activity. In all the fish, coefficient values of FSH cells during stimulation (top) were significantly higher than basal levels. In comparison, in stimulated LH cells of the same fish (bottom), the coefficient values were lower and, in 2/6 fish, the response was not significant (one-way ANOVA, * $p<0.05$, ** $p<0.001$).

(f) The mean cross-correlation coefficient values in each cell type reveal that only FSH cells were significantly affected by CCK stimulation (one-way ANOVA, * $p<0.05$, ** $p<0.001$).

(g) The percentage of active cells (i.e., a coefficient value higher than the 80 percentiles of basal levels) during CCK stimulation is significantly higher in FSH cells compared to LH cells. While in all the fish, 100% of the FSH cells responded to CCK, in only half of the fish LH cells responded. Each dot represents one fish (unpaired *t*-test, * $p<0.05$, ** $p<0.001$).

Differential calcium response underlies differential hormone secretion

The calcium response observed in LH and FSH cells upon GnRH and CCK stimulation, respectively, indicates a differential stimulatory effect of the neuropeptides on the cells. To determine the functional outcome of the stimulation, the effect of these neuropeptides on LH and FSH secretion was examined. For that, we collected the medium perfused through our *ex vivo* system and measured LH and FSH levels (Fig. 2b) while monitoring the calcium activity of the cells. As expected, the calcium response to GnRH in LH cells was followed by a significant rise in LH secretion (Fig. 4a). In contrast, FSH cell elicited a low calcium rise in part of the cells with no significant hormonal secretion in response to GnRH treatment (n=5). Conversely, the application of CCK elicited a significant calcium rise in FSH cells followed by an elevation of FSH concentration in the medium, whereas in LH cells no significant effect was observed (n=5; Fig. 4b). These results, which indicate that the specific calcium response underlies differential gonadotropin secretion, were reproduced *in vivo*, as CCK but not GnRH injection increased the expression and secretion of FSH (Fig. 4c and d). The only observed effect of GnRH was on LH expression in the pituitary (Supplement Figure 4). Although coordinated, high amplitude calcium rises to GnRH and CCK are likely critical for LH and CCK secretions, respectively, we cannot rule out that sparse, low amplitude calcium responses observed in GnRH-stimulated FSH cells (Fig. 2) and CCK-stimulated LH cells (Fig. 3) would regulate other calcium-dependent functions (29).

Taken together, these results suggest that GnRH and CCK specifically activate calcium-dependent secretion in LH and FSH cells, respectively, and induce the differential release of these gonadotropins from the pituitary gland.

a

GnRH-induced cell activity and hormone secretion *ex vivo*

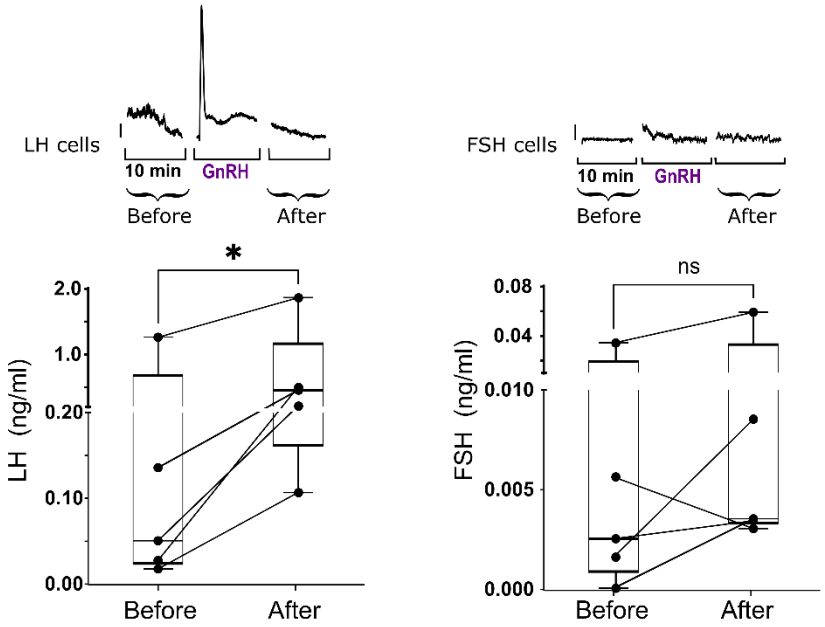

b

CCK-induced cell activity and hormone secretion *ex vivo*

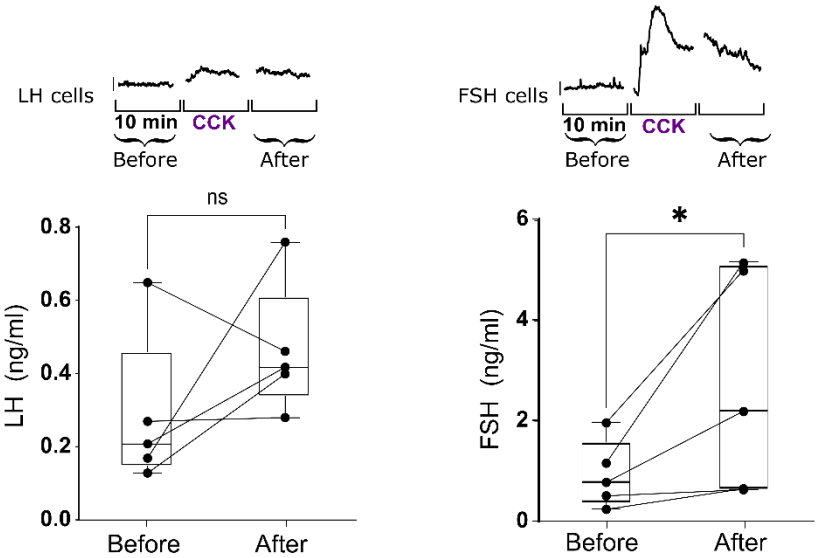

C

transcriptional response to CCK and GnRH in vivo

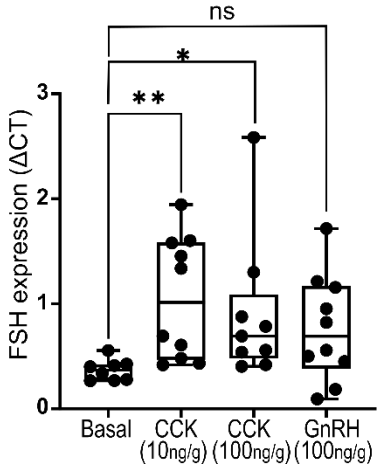

d

FSH secretion in response to CCK and GnRH in vivo

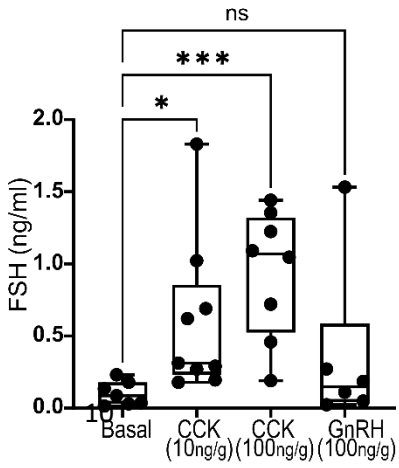

Figure 4. The stimulated calcium activity of LH and FSH cells is associated with hormone secretion

(a and b) Top: Graphs showing mean calcium trace of 10 LH cells (left panel) or FSH cells (right panel) from consecutive imaging sessions before, during, and after the application of the stimulus (GnRH or CCK). Bottom: Secretion of LH or FSH before or after GnRH (a) or CCK (b) stimulation. Compared to basal levels, GnRH increased LH secretion, whereas CCK increased FSH secretion (dots from the same imaged pituitaries are connected with a line; n=5, 3 females and 2 males).

(c) Two hours after injection into live fish (n=10, 5 females and 5 males), CCK, but not GnRH, significantly increased the transcription of FSH in the pituitary (see Supplementary Fig. 4 for LH transcription; one-way ANOVA, * $p<0.05$, ** $p<0.001$).

(d) FSH plasma levels increased significantly in a dose dependent manner after CCK injection (n=10, 5 females and 5 males), whereas GnRH injection did not affect FSH secretion (one-way ANOVA, * $p<0.05$, ** $p<0.001$).

Discussion

GnRH has long been considered the common stimulator of gonadotropin secretion in vertebrates. However, accumulating evidence in several mammalian species for GnRH-independent FSH secretion has brought this regulatory role of GnRH into question (30-33). Moreover, in fish, normal ovarian development in hypophysiotropic GnRH loss-of-function mutants (15, 34) further highlights the existence of an unknown FSH regulator other than GnRH. Here, by combining transcriptomics and calcium imaging *in vivo*, we reveal that in fish, differential gonadotropin secretion is regulated by specialized neuropeptides. We show that GnRH predominantly controls LH secretion and identified, for the first time, CCK as the long-sought hypothalamic FSH secretagogue. Our results indicate that during evolution, fish gonadotrophs were not only segregated into two different populations, but were also placed under the control of two distinct neuropeptides. This has provided a dedicated hypothalamic circuit for the control of folliculogenesis, thereby directly linking the metabolic status of the fish to its reproductive state (Fig. 5).

Unlike mammals, the life histories of many fish species include long periods, lasting months or even years, of folliculogenesis, culminating in a short spawning period. Because of the strict temporal separation between the two processes and the highly stereotyped roles of FSH and LH in controlling folliculogenesis and ovulation in fish (15, 16, 35), during prolonged periods the gonadal activity depends predominantly on FSH secretion. Such temporal separation between the requirements of the two gonadotropins may have provided sufficient evolutionary pressure for the separation of FSH and LH into distinct cell populations and allowed for the cellular specialization of each subpopulation, as reflected by their distinct characteristic ultrastructure and network properties (25).

Here, we show that the specialization of fish gonadotrophs has been accompanied by the emergence of distinct hypothalamic control of each gonadotroph type by two dedicated neuropeptide circuits. From an evolutionary perspective, this dual neuropeptide control serves the unique demands of the life history of oviparous species. Our data suggest that in fish, specific hypothalamic subpopulations have developed to integrate metabolic cues, such as food abundance and somatic condition, to induce the energetically-costly process of folliculogenesis via CCK secretion. By contrast, spawning-relevant signals, such as mate availability and optimal conditions for offspring survival, are integrated to activate the specialized circuit controlling ovulation through release of GnRH.

Our identification of CCK-producing axons innervating the zebrafish pituitary suggest a predominantly central CCK-dependent control of FSH release. Similar innervation was observed in ancient jawless fish such as lamprey (24) and modern teleosts such as the goldfish (36). Modern

oviparous tetrapods were also shown to express the CCK receptor in their pituitary glands (37), indicating that this regulatory circuit may be evolutionarily conserved and common to oviparous vertebrates. However, since CCK is produced in the gut as well as in the central nervous system, we cannot rule out circulating CCK as a possible activator of FSH cells. Nevertheless, the direct innervation of CCK terminals into the pituitary gland and the concomitant increase of CCK in the gut and in the brain in response to feeding (38-40) suggest that the two sources of CCK are interconnected. In this context, the vagal nerve may serve as a possible gut-brain communication route, as it was shown to relay satiety signals to the hypothalamus via CCK (41, 42), thus forming a parasympathetic regulatory loop onto the hypothalamo-pituitary-gonadal axis.

Overall, our findings proposes an updated view of the regulation of gonadal function in fish, in which separate neuronal circuits evolved to control gonad development and ovulation. In addition to the insight into the evolution and function of the reproductive axis in oviparous animals, these findings are also of particular importance in the context of aquaculture, which has become the dominant supplier of fish for human consumption in the face of declining yields from wild fisheries (43, 44). With the identification of the CCK circuit as a regulator of folliculogenesis, novel tools targeting this pathway can now be designed to manipulate gonadal development and overcome challenges in gamete production and the control of puberty onset in farmed fish (4, 45).

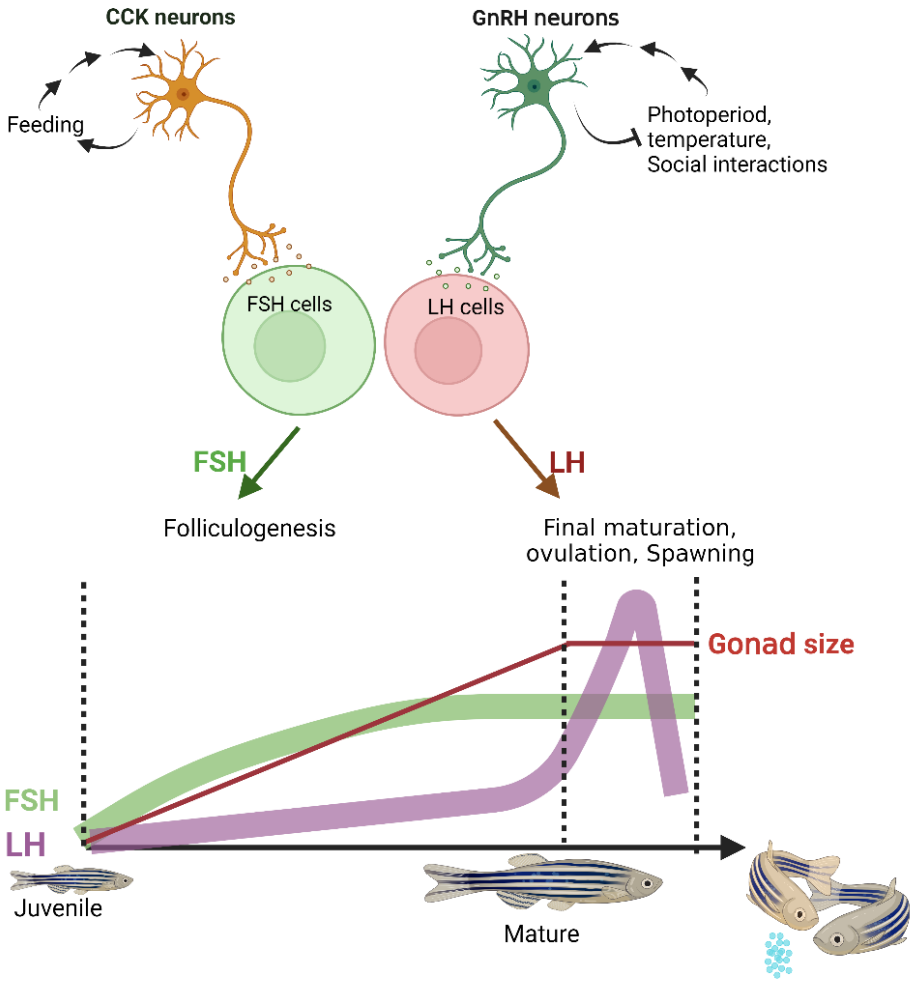

Figure 5. A model summarizing the two suggested regulatory axes controlling fish reproduction.

Whereas satiety-regulated CCK neurons activate FSH cells, which control folliculogenesis, LH cells are regulated by GnRH neurons that are activated by photoperiod, temperature, and behavior, eventually leading to final maturation and ovulation. Bottom graph schematically represents the relative timescale of the two processes and the associated gonadotropin levels.

3. Methods

Experimental design

To identify the regulatory mechanism that allows the differential secretory activity of LH and FSH cells, we took advantage of the fact that in fish, these gonadotropic hormones are produced by two separated cell populations. Using the well-established model organism the zebrafish, we simultaneously monitored the activity of LH and FSH cells in a triple transgenic fish that expresses RCaMP2 under the regulation of both LH and FSH promoters, together with GFP under the regulation of FSH promoter. Because gonadotrophs control reproductive physiology, we used sexually mature fish that were at least six months old, contained mature gonads and exhibited reproductive behaviour. In each assay, the sex of each fish was determined by dissecting the gonads and identifying the morphology of eggs or sperm. We first characterised the *in vivo* calcium activity of the cells in an intact physiological environment. Then, we stimulated the pituitary by either GnRH or CCK and measured calcium activity. For that, we used isolated brains containing the pituitary, since no difference was observed in calcium activity of isolated pituitary or isolated brain and pituitary. Experimental units were either individual fish or GtH cells, depending on the experiment.

Sample size and replication

Sample size varied between experiments, depending on the number of transgenic fish allocated for each experiment. The minimum sample size was three from each sex, i.e. six fish.

Data inclusion/exclusion criteria

Fish were excluded from analysis if the fish showed no calcium activity or if tissue movements during the full recording session prevented reliable calcium analysis. Data or samples were not excluded from analysis for other reasons.

Randomization

Fish used for the experiments were randomly selected and randomly assigned to experimental groups. All GtH cells that could be detected in the selected fish were used for the analysis and, thus, there was no requirement for randomization of cell selection.

Blinding

During experimentation and data acquisition, blinding was not applied to ensure tractability. Calcium data were quantified using a computational pipeline applied equally to all samples.

Animals

All experiments were approved by the Animal Welfare and Ethical Review Body of Languedoc-Roussillon (APAFIS#745-2015060114396791 v3) and by the Experimentation Ethics Committee of the Hebrew University of Jerusalem (research number: AG-17-15126, Date: April 30, 2017). Zebrafish were housed according to standard conditions. Fertilized eggs were incubated at 28.5°C in E3 medium. For

the current study, the transgenic line Tg(LH&FSH:RCaMP2) was generated by microinjection of the constructs to embryos. Other transgenic lines used were Tg(FSH:GFP) and Tg(GnRH:GFP) and Tg(LH:RFP, FSH:GFP) (46).

Plasmid construction

All expression plasmids were generated using the Tol2kit (47) and Gateway system (Invitrogen). Briefly, entry clones were generated by addition of appropriate adaptors to DNA fragments via polymerase chain reaction (PCR) amplification. Amplicons were then recombined into donor vectors using BP recombination. A 5'-entry clone (p5E), a middle entry clone (pME), and a 3'-entry clone (p3E) were then recombined through an LR reaction into an expression vector carrying tol2-recognition sequences and either an mCherry or a GFP heart marker (pDestTol2CG). The LH and FSH promoters (46) were cloned from Nile tilapia genomic DNA and inserted into pDONRP4-P1R to generate p5'-LH and p5'-FSH. R-CaMP2 (48) was a gift from H. Bito (University of Tokyo) and was cloned into pDONR221 to generate pME-R-CaMP2. For GFP expression, the middle clone pME-EGFP was used. The expression vectors containing p5E-**LH**:PME-R-CaMP2:p3E-PolyA (red heart marker) and p5E-**FSH**:PME-R-CaMP2:p3E-PolyA (green heart marker) were co-injected to create Tg(LH&FSH:CaMP2) fish, which were later crossed with Tg(FSH:GFP) fish to generate the triple transgenic fish.

***In vivo* calcium imaging**

Adult fish were anesthetized using 0.6 µM tricaine and immobilized by IP injection of 10 µl α-tubocurarine (5 mM; Sigma-Aldrich). To expose the pituitary (Fig. 1b), the jaw of the fish containing the dentary and part of the articular bones, together with a small slice from the mucosa overlying the palate, were removed by blunt dissection under a stereomicroscope. The fish was then placed in a modified chamber, where the hyoid bone was gently pushed backward using a thin silver wire. A tube with a constant flow of fresh system water was placed in the jaw cavity In front of the gills. Heartbeat was monitored during calcium imaging as an indicator of viability. Each imaging session lasted 10 minutes and was repeated several times for each fish.

Calcium imaging was performed using a FVMPE RS two-photon microscope (Olympus) setup with an InSight X3 femtosecond-pulsed infrared laser (Spectra-Physics) and a 25×, numerical aperture 1.05 water-immersion objective (XLPLN25XWMP2, Olympus). The laser wavelength was tuned to 940 nm for GFP or to 1040 nm for R-CaMP2. Calcium signals were recorded by time-lapse acquisition using galvanometric scanning mode and conventional raster scanning with a frequency up to 10 Hz.

***Ex vivo* calcium imaging**

Adult fish were euthanised using ice-cold water and decapitated. The head was transferred to ice-cold ACSF (124 mM NaCl, 3 mM KCl, 2 mM $CaCl_2$, 2 mM $MgSO_4$, 1.25 mM NaH_2PO_4, 26 mM $NaHCO_3$, and 10 mM glucose (pH 7.2)) perfused with 5% CO_2 and 95% O_2. The heads were further dissected under a stereomicroscope. The ventral side of the head, includes jaw, gills and mucus, was removed using fine forceps and microscissors, the optic nerves were cut and the eyes were removed. Next, the bone at the base of the skull that covers the pituitary (sella turcica) was removed using fine forceps. The head was then placed in a dedicated chamber (Fig. 2b) and stabilized with a slice anchor. The chamber had one inlet and one outlet, allowing for a constant flow of ACSF at a rate of 1 ml/minute, and an additional inlet that was placed in proximity to the tissue for injections of stimuli. The total volume of ACSF in the chamber was 3 ml.

Imaging was performed in an inverted confocal fluorescent microscope (Leica SP8). R-CaMP2 activity was imaged at a speed of 4-10 Hz using the resonant scanner. The laser wavelength was 540 nm and

the emission band was 630 nm. Images were taken using the ×20 objective. Each imaging session lasted 10 minutes. Before and after each session, the tissue was imaged once for GFP (excitation, 488 nm and emission, 530 nm) and R-CaMP2 (540 nm and 590 nm) in two separated channels. Images were processed using the Fiji program (49) for resolution using the Gaussian Blur filter and for motion correction using the moco plugin (50).

To measure hormone secretion in response to GnRH or CCK stimulation, the medium was collected through the chamber outlet during the entire imaging session (10 ml per session in total). Each pituitary was imaged three times for 10 minutes: before, during and after stimulation. The stimulus was applied manually as a pulse of 300 µl of 30 µg/µl peptide during the first 30 seconds of the imaging session. Hormones were measured in the fractions before and after stimulation using ELISA for another Cyprinid, namely carp, which had been previously shown to be suitable for zebrafish (24).

Analysis of Ca_2^+ imaging data

A composite of GFP-positive and RCaMP-positive cells was created to distinguish between LH and FSH cells. Regions of interest corresponding to each cell in the imaged plane were manually drawn using Fiji. Two separated ROI sets were created, one for FSH cells (GFP-positive) and one for LH cells (R-CaMP2-positive and GFP-negative). Using the Fiji ROI manager, two dataset were created: a data sheet containing the mean grey values in each frame during the complete image sequence, and a data sheet containing the ROI centroids. Sheets and images were then processed using MATLAB R2017a.

Traces were normalized using the equation $\Delta F = \frac{Ft}{F0} - 1$, where $F0$ is the lowest value in the means calculated from every N frames in the complete trace (N= sampling frequency*5). When the sampling rate was higher than 4 Hz, we applied a low pass filter with a cut-off frequency of 2/ (sampling frequency /2).

Analysis of pairwise correlations and delay between cells

Cross-correlation coefficients represent the maximum coefficient value between the traces of each cell and the trace of a reference ROI. From each set of traces, we obtained cross-correlation sequence ranges from -maxlag to maxlag and the values were normalized such that autocorrelations at 0 lag equalled 1. The delay between the trace of each cell to that of a reference ROI is the time corresponding to the maximum of the cross-correlation sequence. Cross-correlation coefficient values and delay values are represented in a dot plot superimposed on the cells according to their centroid values. In all images, the reference cell is shown in pink. For violin plots, maximum cross-correlation coefficient values were further visualized and analysed for statistical significance using Prism 9 (GraphPad, San Diego, CA).

HCR for CCKR and immunostaining of CCK

Staining was performed on whole head slices, as previously described (51). Briefly, whole heads were fixed overnight in 4% paraformaldehyde (PFA) and then decalcified for 4–7 days in 0.5 M EDTA at 4°C. Subsequently, heads were cryoprotected in 30% (wt/vol) sucrose, frozen in an OCT embedding compound and cryosectioned at a thickness of 15 µm. For immunostaining, head sections from transgenic zebrafish tg(GnRH:GFP) and tg(FSH:GFP) (51) were blocked with 5% normal goat serum for 1 h to reduce non-specific reactions. They were then incubated with rabbit anti-cholecystokinin (26-33) (CCK-8) antibody (diluted 1:1000, Merck, C2581) for 16 h at 4°C. The same antibody had been previously used to mark CCK-positive cells in the gut of the red drum fish (52). Antibodies were diluted in PBS with 1% BSA and 0.3% Triton X-100. The slides were rinsed three times with PBS for 5 min and

were incubated for 2 h at room temperature with goat anti-rabbit antibodies conjugated to Alexa674 fluorophore. HCR staining was performed according to the HCR RNA-FISH protocol for fresh-frozen or fixed-frozen tissue sections (53) (Molecular Instrument) on double-labelled transgenic fish Tg(LH:RFP, FSH:GFP). The detection stage was performed with probes against CCKR-like RNA (XM_017357750.2) and the amplification stage was performed using the 647 nm amplifier fluorophores. Sections were then counterstained with DAPI nuclear staining. After washing, slides were mounted with anti-fade solution (2% propyl gallate, 75% glycerol, in PBS) and imaged by confocal microscopy.

In vivo assay for CCK and GnRH injections

Six-month-old zebrafish (5 males and 5 females) were injected intraperitoneally with the following: 1) fish CCK peptide [(D-Y[SO3H]-L-G-W-M-D-F-NH2), synthesized by GL Biochem] at a concentration of 10 ng/g or 100 ng/g body weight, 2) salmon GnRH analogue [(D-Ala6,Pro9-Net)-mammalian GnRH (Bachem Inc., Torrance, CA) at a concentration of 100 ng/g body weight, 3) similar volumes of saline. Two hours post-injection, the fish were sedated using MS-222, bled from the heart as previously described (54), and decapitated. Pituitaries were dissected under a stereomicroscope and placed in Total RNA Isolation Reagent (Trizol). From each fish, between 15 µl and 20 µl of blood was collected. The blood was centrifuged at 970 × g 30 min and the plasma was separated and stored at −20°C. LH and FSH expression in the pituitary was measured using real-time PCR. RNA extraction, reverse transcription of RNA and real-time PCR were carried out as previously described (17). FSH secretion was measured in the plasma using ELISA for another Cyprinidae, carp, which had been previously shown to be suitable for zebrafish (55).

Statistical analysis

Statistical analysis was performed using Prism 9 software (GraphPad). Whiskers on bar plots represent mean ± SEM**.** In violin plots, middle line represents the median, whereas the bottom and top lines represent the lower and upper quartiles, respectively. Basal and stimulated activity levels of the same cell population were compared using two-tailed unpaired *t*-test**.** For the mean of cross-correlation coefficients in the different cell types and the number of active cells in different fish, the datasets were tested for equal variances (using Bartlett's test) and normality (using D'Agostino and Pearson's test or Shapiro-Wilk test for smaller datasets). Dataset pairs that exhibited equal variances and normal distribution were compared using two-tailed unpaired *t*-test (for two sets). For datasets with more than two sets we used one-way analysis of variance (ANOVA), followed by Tukey-Kramer test. Datasets with different variances and/or non-Gaussian distributions were tested using two-tailed Mann-Whitney's test (for two sets) or Brown-Forsythe's one-way ANOVA, followed by Dunnett's T3 multiple comparisons test. To compare levels of secreted hormone in the *ex vivo* assay, the one-tailed paired *t*-test (Wilcoxon test) was performed, as the sample size was lower than 10. To compare the datasets of the *in vivo* assay of CCK and GnRH injections, a nonparametric one-way ANOVA test (Kruskal-Wallis test) was used, as the datasets failed the Bartlett's test of equal variance. Significance was imparted at $P < 0.05$ (n.s., nonsignificant; *$P < 0.05$; **$P < 0.01$; ***$P < 0.001$; ****$P < 0.0001$).

Acknowledgments

The writers would like to acknowledge the contribution of Mr Antony Pinot from the Mollard lab for its help in operating the two-photon microscopy, Einat Zelinger and Daniel Waiger from the CSI Center for Scientific Imaging Faculty of Agriculture for, for their help in guidance in operating the confocal microscopy. The authors acknowledge the IPAM-BCM Platform, member of the national infrastructure France-BioImaging supported by the French National Research Agency (ANR-10-INBS-04). The Israel Science

Foundation (ISF) support (grant number 1540/17), and the U.S.-Israel Binational Science Foundation (Joint Funding Research Grants # NSF-BSF-1947541)

References

1. Ashworth CJ, Toma LM, Hunter MG. Nutritional effects on oocyte and embryo development in mammals: implications for reproductive efficiency and environmental sustainability. Philos Trans R Soc Lond B Biol Sci. 2009;364(1534):3351-61.
2. Torre SD, Benedusi V, Fontana R, Maggi A. Energy metabolism and fertility—a balance preserved for female health. Nature Reviews Endocrinology. 2014;10(1):13-23.
3. Mobley KB, Aykanat T, Czorlich Y, House A, Kurko J, Miettinen A, et al. Maturation in Atlantic salmon (Salmo salar, Salmonidae): a synthesis of ecological, genetic, and molecular processes. Reviews in Fish Biology and Fisheries. 2021;31(3):523-71.
4. Taranger GL, Carrillo M, Schulz RW, Fontaine P, Zanuy S, Felip A, et al. Control of puberty in farmed fish. Gen Comp Endocrinol. 2010;165(3):483-515.
5. Mylonas CC, Mitrizakis N, Castaldo CA, Cerviño CP, Papadaki M, Sigelaki I. Reproduction of hatchery-produced meagre Argyrosomus regius in captivity II. Hormonal induction of spawning and monitoring of spawning kinetics, egg production and egg quality. Aquaculture. 2013;414-415:318-27.
6. Sarih S, Djellata A, La Barbera A, Fernández-Palacios Vallejo H, Roo J, Izquierdo M, et al. High-quality spontaneous spawning in greater amberjack (Seriola dumerili, Risso 1810) and its comparison with GnRHa implants or injections. Aquaculture Research. 2018;49(10):3442-50.
7. Guzmán JM, Ramos J, Mylonas CC, Mañanós EL. Spawning performance and plasma levels of GnRHa and sex steroids in cultured female Senegalese sole (Solea senegalensis) treated with different GnRHa-delivery systems. Aquaculture. 2009;291(3):200-9.
8. Corriero A, Medina A, Mylonas CC, Bridges CR, Santamaria N, Deflorio M, et al. Proliferation and apoptosis of male germ cells in captive Atlantic bluefin tuna (Thunnus thynnus L.) treated with gonadotropin-releasing hormone agonist (GnRHa). Animal Reproduction Science. 2009;116(3):346-57.
9. Kagawa H, Tanaka H, Ohta H, Unuma T, Nomura K. The first success of glass eel production in the world: basic biology on fish reproduction advances new applied technology in aquaculture. Fish Physiology and Biochemistry. 2005;31(2):193.
10. Drori S, Ofir M, Levavi-Sivan B, Yaron Z. Spawning Induction in common carp (*Cyprinus Carpio*) using pituitary extract or GnRH superactive analog combined with metoclopramide - analysis of hormone profile, progress of oocyte maturation and dependence on temperature. Aquaculture. 1994;119(4):393-407.
11. Belchetz PE, Plant TM, Nakai Y, Keogh EJ, Knobil E. Hypophysial Responses to Continuous and Intermittent Delivery of Hypothalamic Gonadotropin-Releasing Hormone. Science. 1978;202(4368):631-3.
12. Savoy-Moore R, Swartz K. Several GnRH stimulation frequencies differentially release FSH and LH from isolated, perfused rat anterior pituitary cells. Regulation of Ovarian and Testicular Function: Springer; 1987. p. 641-5.
13. Stamatiades GA, Kaiser UB. Gonadotropin regulation by pulsatile GnRH: Signaling and gene expression. Molecular and cellular endocrinology. 2018;463:131-41.
14. Thompson IR, Kaiser UB. GnRH pulse frequency-dependent differential regulation of LH and FSH gene expression. Molecular and cellular endocrinology. 2014;385(1-2):28-35.
15. Takahashi A, Kanda S, Abe T, Oka Y. Evolution of the Hypothalamic-Pituitary-Gonadal Axis Regulation in Vertebrates Revealed by Knockout Medaka. Endocrinology. 2016;157(10):3994-4002.
16. Zhang Z, Lau S-W, Zhang L, Ge W. Disruption of Zebrafish Follicle-Stimulating Hormone Receptor (fshr) But Not Luteinizing Hormone Receptor (lhcgr) Gene by TALEN Leads to Failed Follicle Activation in Females Followed by Sexual Reversal to Males. Endocrinology. 2015;156(10):3747-62.
17. Biran J, Ben-Dor S, Levavi-Sivan B. Molecular identification and functional characterization of the kisspeptin/kisspeptin receptor system in lower vertebrates. Biology of reproduction. 2008;79(4):776-86.
18. Ogawa S, Sivalingam M, Biran J, Golan M, Anthonysamy RS, Levavi-Sivan B, et al. Distribution of LPXRFa, a gonadotropin-inhibitory hormone ortholog peptide, and LPXRFa receptor in the brain and pituitary of the tilapia. The Journal of comparative neurology. 2016;524(14):2753-75.
19. Biran J, Golan M, Mizrahi N, Ogawa S, Parhar IS, Levavi-Sivan B. LPXRFa, the Piscine Ortholog of GnIH, and LPXRF Receptor Positively Regulate Gonadotropin Secretion in Tilapia (Oreochromis niloticus). Endocrinology. 2014;155(11):4391-401.
20. Tsutsui K, Ubuka T, Bentley GE, Kriegsfeld LJ. Gonadotropin-inhibitory hormone (GnIH): discovery, progress and prospect. Gen Comp Endocrinol. 2012;177(3):305-14.

21. Biran J, Golan M, Mizrahi N, Ogawa S, Parhar IS, Levavi-Sivan B. Direct regulation of gonadotropin release by neurokinin B in tilapia (Oreochromis niloticus). Endocrinology. 2014;155(12):4831-42.
22. Cohen Y, Hausken K, Bonfil Y, Gutnick M, Levavi-Sivan B. Spexin and a Novel Cichlid-Specific Spexin Paralog Both Inhibit FSH and LH Through a Specific Galanin Receptor (Galr2b) in Tilapia. Front Endocrinol (Lausanne). 2020;11:71.
23. Himick BA, Peter RE. CCK/gastrin-like immunoreactivity in brain and gut, and CCK suppression of feeding in goldfish. The American journal of physiology. 1994;267(3 Pt 2):R841-51.
24. Sobrido-Cameán D, Yáñez-Guerra LA, Robledo D, López-Varela E, Rodicio MC, Elphick MR, et al. Cholecystokinin in the central nervous system of the sea lamprey Petromyzon marinus: precursor identification and neuroanatomical relationships with other neuronal signalling systems. Brain Struct Funct. 2020;225(1):249-84.
25. Golan M, Martin AO, Mollard P, Levavi-Sivan B. Anatomical and functional gonadotrope networks in the teleost pituitary. Scientific reports. 2016;6:23777.
26. Inoue M, Takeuchi A, Horigane S, Ohkura M, Gengyo-Ando K, Fujii H, et al. Rational design of a high-affinity, fast, red calcium indicator R-CaMP2. Nat Methods.12(1):64-70.
27. Zohar Y, Mylonas CC. Endocrine manipulations of spawning in cultured fish: from hormones to genes. Aquaculture. 2001;197(1-4):99-136.
28. Hollander-Cohen L, Golan M, Levavi-Sivan B. Differential Regulation of Gonadotropins as Revealed by Transcriptomes of Distinct LH and FSH Cells of Fish Pituitary. Int J Mol Sci. 2021;22(12).
29. Berridge MJ. The Inositol Trisphosphate/Calcium Signaling Pathway in Health and Disease. Physiol Rev. 2016;96(4):1261-96.
30. McCann SM, Karanth S, Mastronardi CA, Dees WL, Childs G, Miller B, et al. Control of Gonadotropin Secretion by Follicle-Stimulating Hormone-Releasing Factor, Luteinizing Hormone-Releasing Hormone, and Leptin. Archives of Medical Research. 2001;32(6):476-85.
31. Padmanabhan V, McFadden K, Mauger DT, Karsch FJ, Midgley AR, Jr. Neuroendocrine Control of Follicle-Stimulating Hormone (FSH) Secretion. I. Direct Evidence for Separate Episodic and Basal Components of FSH Secretion1. Endocrinology. 1997;138(1):424-32.
32. Culler MD, Negro-Vilar A. Pulsatile follicle-stimulating hormone secretion is independent of luteinizing hormone-releasing hormone (LHRH): pulsatile replacement of LHRH bioactivity in LHRH-immunoneutralized rats. Endocrinology. 1987;120(5):2011-21.
33. Pau KY, Gliessman PM, Oyama T, Spies HG. Disruption of GnRH pulses by anti-GnRH serum and phentolamine obliterates pulsatile LH but not FSH secretion in ovariectomized rabbits. Neuroendocrinology. 1991;53(4):382-91.
34. Marvel M, Spicer OS, Wong TT, Zmora N, Zohar Y. Knockout of the Gnrh genes in zebrafish: effects on reproduction and potential compensation by reproductive and feeding-related neuropeptides. Biology of reproduction. 2018;99(3):565-77.
35. Chu L, Li J, Liu Y, Hu W, Cheng CH. Targeted gene disruption in zebrafish reveals noncanonical functions of LH signaling in reproduction. Molecular endocrinology (Baltimore, Md). 2014;28(11):1785-95.
36. Himick BA, Peter RE. CCK/gastrin-like immunoreactivity in brain and gut, and CCK suppression of feeding in goldfish. American Journal of Physiology-Regulatory, Integrative and Comparative Physiology. 1994;267(3):R841-R51.
37. Wan Y, Deng Q, Zhou Z, Deng Y, Zhang J, Li J, et al. Cholecystokinin (CCK) and its receptors (CCK1R and CCK2R) in chickens: functional analysis and tissue expression. Poultry Science. 2023;102(1):102273.
38. Zhang X, Tang N, Qi J, Wang S, Hao J, Wu Y, et al. CCK reduces the food intake mainly through CCK1R in Siberian sturgeon (Acipenser baerii Brandt). Scientific reports. 2017;7(1):12413.
39. Gomes AS, Lygre E, Harboe T, Zimmermann F, Jordal A-EO, Hamre K, et al. The role of cholecystokinin and peptide YY in feed intake in Atlantic halibut (Hippoglossus hippoglossus) larvae. Neuropeptides. 2022;91:102202.
40. D'Agostino G, Lyons DJ, Cristiano C, Burke LK, Madara JC, Campbell JN, et al. Appetite controlled by a cholecystokinin nucleus of the solitary tract to hypothalamus neurocircuit. eLife. 2016;5:e12225.
41. Borgmann D, Ciglieri E, Biglari N, Brandt C, Cremer AL, Backes H, et al. Gut-brain communication by distinct sensory neurons differently controls feeding and glucose metabolism. Cell Metabolism. 2021;33(7):1466-82.e7.
42. Clemmensen C, Müller TD, Woods SC, Berthoud H-R, Seeley RJ, Tschöp MH. Gut-Brain Cross-Talk in Metabolic Control. Cell. 2017;168(5):758-74.
43. Froehlich HE, Runge CA, Gentry RR, Gaines SD, Halpern BS. Comparative terrestrial feed and land use of an aquaculture-dominant world. Proceedings of the National Academy of Sciences. 2018;115(20):5295-300.
44. Anderson JL, Asche F, Garlock T, Chu J. Aquaculture: Its role in the future of food. World agricultural resources and food security: Emerald Publishing Limited; 2017.

45. Zohar Y. Endocrinology and fish farming: Aspects in reproduction, growth, and smoltification. Fish Physiology and Biochemistry. 1989;7(1):395-405.
46. Golan M, Biran J, Levavi-Sivan B. A novel model for development, organization and function of gonadotropes in fish pituitary. Frontiers in Endocrinology. 2014;5:182.
47. Kwan KM, Fujimoto E, Grabher C, Mangum BD, Hardy ME, Campbell DS, et al. The Tol2kit: A multisite gateway-based construction kit for Tol2 transposon transgenesis constructs. Developmental Dynamics. 2007;236(11):3088-99.
48. Dana H, Mohar B, Sun Y, Narayan S, Gordus A, Hasseman JP, et al. Sensitive red protein calcium indicators for imaging neural activity. eLife. 2016;5:e12727.
49. Schindelin J, Arganda-Carreras I, Frise E, Kaynig V, Longair M, Pietzsch T, et al. Fiji: an open-source platform for biological-image analysis. Nat Methods. 2012;9(7):676-82.
50. Dubbs A, Guevara J, Yuste R. moco: Fast Motion Correction for Calcium Imaging. Front Neuroinform. 2016;10:6-.
51. Golan M, Zelinger E, Zohar Y, Levavi-Sivan B. Architecture of GnRH-Gonadotrope-Vasculature Reveals a Dual Mode of Gonadotropin Regulation in Fish. Endocrinology. 2015;156(11):4163-73.
52. Webb KA, Jr., Khan IA, Nunez BS, Rønnestad I, Holt GJ. Cholecystokinin: molecular cloning and immunohistochemical localization in the gastrointestinal tract of larval red drum, Sciaenops ocellatus (L.). Gen Comp Endocrinol. 2010;166(1):152-9.
53. Choi HMT, Schwarzkopf M, Fornace ME, Acharya A, Artavanis G, Stegmaier J, et al. Third-generation in situ hybridization chain reaction: multiplexed, quantitative, sensitive, versatile, robust. Development. 2018;145(12).
54. Biran J, Palevitch O, Ben-Dor S, Levavi Sivan B. Neurokinin B and neurokinin B receptor: a novel system involved in controlling fish reproduction. PNAS. 2012;109(26):10269-74.
55. Hollander-Cohen L, Golan M, Aizen J, Shpilman M, Levavi-Sivan B. Characterization of carp gonadotropins: Structure, annual profile, and carp and zebrafish pituitary topographic organization. Gen Comp Endocrinol. 2018;264:28-38.